Experimental Study of Neutral Configuration Effects on Internal and External Fault Detection in Induction Motors

Nacer Merabet*[ID], Fatima Babaa[ID], Abderrahim Touil[ID], Oualid Abd Elghani Chibani[ID]

Electrical Engineering Laboratory of Constantine, Université Frères Mentouri Constantine 1, Constantine 25017, Algeria

Corresponding Author Email: nacer.merabet1@doc.umc.edu.dz

ABSTRACT

This paper investigates the impact of neutral configuration on the detection and diagnosis of unbalance in induction motors, a key factor in maintaining their efficiency and operational lifespan. Induction motors, while highly efficient, are prone to unbalances caused by internal faults (rotor, stator, or winding defects) or external disturbances (voltage asymmetries or frequency variations). The research explores how different neutral configurations influence the accuracy and reliability of electrical measurements and the effectiveness of monitoring systems in identifying anomalies. Experimental results demonstrate that neutral configurations significantly affect the detection of both internal and external unbalances. Some configurations enhance early fault identification, while others improve immunity to external disturbances. These findings provide critical insights for optimizing motor monitoring systems, advancing predictive maintenance strategies, and extending equipment lifespan. The study highlights the importance of selecting appropriate neutral configurations to enhance diagnostic accuracy and ensure reliable motor performance in industrial applications, offering practical implications for improving operational efficiency and reducing maintenance costs.

1. INTRODUCTION

Induction motors (IM) are electromechanical devices widely used in industry to convert electrical energy into mechanical energy [1, 2]. Used in numerous industrial applications, they can be subject to both internal and external failures that affect their performance and durability. Internal failures include issues such as short circuits [3] in the stator or rotor windings [4], phase unbalances [5], mechanical defects (bearing wear, excessive vibrations) [6, 7], and overheating due to inadequate cooling. These failures can lead to efficiency losses, premature breakdowns, or irreversible damage to internal components [8, 9]. External failures, on the other hand, are related to factors such as asymmetric voltages or frequency variations in the electrical grid, overloads or load fluctuations, and adverse environmental conditions (humidity, dust, extreme temperatures) [10]. Additionally, inadequate maintenance or improper installation can exacerbate these problems [6]. These failures can have serious consequences, such as frequent shutdowns, increased energy costs, expensive repairs, or even total motor failure [4]. As a fault external to the machine, we distinguish voltage unbalance. It occurs when the voltages of the three phases are unequal in magnitude or phase, disrupting the operation of equipment [11]. The consequences include increased phase currents, reduced torque, excessive vibration and noise, reduced fuel efficiency, and in severe cases, damage to motor components [12]. As an internal fault in the machine, we distinguish the

broken rotor bar fault, which results from the mechanical or electrical rupture of certain bars in IM [13]. The causes include mechanical fatigue, shocks, electrical overloads, poor design or manufacturing, electromagnetic unbalances, excessive vibrations, thermal cycles, and material aging [7]. This fault leads to serious consequences, such as torque unbalances, reduced efficiency, overheating of the remaining bars, triggering an avalanche effect that deteriorates adjacent bars, secondary failures (such as damage to bearings or stator insulation) [6], and an increased risk of unexpected machine [14, 15]. The performance of machines is therefore significantly affected by various electrical unbalances, which, if not detected and corrected in time, can lead to reduced efficiency, increased wear on components, and even complete motor failure [11]. One of the key factors influencing the detection and management of these unbalances is the configuration of the neutral point in the electrical system supplying the motor [2, 5]. The neutral point configuration can have a significant impact on the motor's ability to handle unbalances, whether internal or external. In IM, the neutral refers to the common point of the stator windings when connected in a star configuration, which can either be grounded or ungrounded within the electrical system. A grounded neutral is directly connected to the earth or an external neutral conductor, providing enhanced protection against voltage surges and unbalances [16]. It allows unbalanced currents to flow, helping maintain voltage stability and facilitating fault detection to ground, which ensures more reliable motor operation. This

configuration is commonly used in systems requiring greater stability, such as motors powered by a three-phase network. On the other hand, an ungrounded neutral is not connected to the earth or any external neutral conductor, remaining isolated within the system [17]. While it reduces ground leakage currents, it prevents current flow during unbalances or ground faults, leading to floating voltages. This complicates fault detection and unbalance compensation, increasing vibrations, overheating, and accelerating component wear [18]. It is essential to remedy this deficiency, as the correct neutral configuration allows effective monitoring, thereby optimizing motor performance. It also enables early and accurate fault detection, which is essential to ensure long system life, reliability and efficiency.

The aim of this paper is to investigate the impact of neutral configuration on the detection of internal and external unbalances in IM. Through a series of experimental tests, we will analyze how linked and unlinked neutral systems affect the ability to detect unbalances within the machine. Additionally, the motor's response to faults and its overall performance under various load conditions will be evaluated. By comparing these configurations, the research will provide valuable insights into the optimal conditions for motor operation, fault detection, and system stability. The findings of this study will contribute to the development of more efficient monitoring systems and enhanced maintenance strategies, ultimately optimizing the performance and longevity of IM in industrial settings.

2. NEUTRAL SYSTEMS AND THEIR IMPACT ON ASYNCHRONOUS MACHINES

In electrical systems, the configuration of the neutral system plays a vital role in ensuring protection, safety, and operational performance. The neutral system determines how the neutral point is connected to the earth and directly influences the connection and operation of electrical machines, including IM. Two key scenarios arise for asynchronous motors, one where the neutral is connected to the star point of the windings, and another where the neutral is not connected, either linked to the motor frame (yoke) or excluded entirely. Table 1 summarizes their impact on the IM.

Table 1. Comparison of the two configurations

Criterion	Neutral Connected to Star Point	Neutral Not Connected (Linked to Frame)
Electrical Network	TT or TN-S (neutral available)	IT (isolated or impedance earthed neutral)
Safety	Better balancing of phase voltages	Improved fault isolation
Application	Small/medium installations	Industrial or critical environments
Impact on the Motor	Requires neutral for voltage balancing	Less dependent on system voltage balance

2.1 Neutral connected to the star point of the windings

In this configuration, the motor's stator windings are arranged in a star (Y) formation, with the star point connected to the system's neutral. This setup helps balance phase voltages during system asymmetries, thereby reducing unbalance. Additionally, it simplifies motor starting by lowering the voltage across each winding ($1/\sqrt{3}$ of the line voltage), which reduces the starting inrush current caused by resistive torque. This configuration is particularly well-suited to TT and TN-S networks, where a neutral conductor is readily available. It is widely used in small to medium-sized installations, including residential, commercial, and industrial applications, where the neutral connection is easily accessible.

2.2 Neutral not connected to the star point (linked to the motor frame)

In this configuration, the star point of the motor windings remains isolated from the network's neutral, or the stator phases are connected in a delta (Δ) arrangement. Instead, the motor frame (yoke) is connected to the protective earth (PE). This design allows the motor to operate without a direct connection to the network neutral, offering several advantages. It enhances insulation by preventing direct fault currents through the neutral, which increases system robustness. This setup is particularly compatible with isolated or impedance-earthed neutral systems (IT networks), as it minimizes the impact of ground faults. Furthermore, it is highly suited for industrial environments and applications involving power electronics, such as variable frequency drives (VFDs), soft starters, or frequency converters, where a neutral connection is typically unnecessary.

The choice of IM configuration depends on the neutral regime of the electrical network and the specific requirements of the application (Table 1). Connecting the neutral to the star point is ideal for balanced systems with accessible neutral conductors, while isolating the neutral is more suitable for industrial setups prioritizing insulation and robustness. A thorough understanding of these configurations ensures optimal performance, reliability, and adaptability in IM operation.

The neutral point configuration plays a critical role in determining the electromagnetic field distribution and current harmonics in the motor. In a three-phase system, the neutral point can be isolated, grounded, or connected in various ways, each influencing the motor's performance differently. For instance, a grounded neutral point configuration tends to reduce zero-sequence harmonics, as it provides a path for these currents to flow. However, this configuration may also lead to increased electromagnetic interference due to the grounding path. Conversely, an isolated neutral point configuration minimizes electromagnetic interference but can result in higher harmonic distortion due to the absence of a zero-sequence current path.

The influence of neutral point configuration on flux distribution and machine behavior has been extensively investigated in recent studies to provide a well-rounded assessment. For instance, they demonstrated that floating neutral point systems in induction machines exhibit heightened thermal stresses under unbalanced voltage conditions, emphasizing the sensitivity of flux distribution to voltage imbalances [17]. Similarly, other works analyzed the impact of neutral point current control, showing that floating neutral configurations can limit copper losses and fault currents, though they introduce complexity in monitoring [19]. On the other hand, Previous work highlighted the

advantages of bonded neutral points in stabilizing the neutral voltage, which aids in maintaining balanced flux distribution and facilitates fault detection [20]. Complementary findings stressed that small-resistance grounding at the neutral point reduces voltage fluctuations, improving system stability [16]. Others further supported the role of optimized neutral grounding in mitigating geomagnetically induced current effects, reinforcing the safety and voltage control benefits of bonded neutral configurations [16]. This comparative analysis underscores the trade-offs: while floating neutral systems offer benefits in reducing fault current magnitudes and losses, bonded neutral configurations remain preferred for voltage stability and simplified fault management in practical applications.

3. NEUTRAL POINT CONFIGURATION ANALYZING

The neutral point in a three-phase system is crucial for the efficient operation of IM. It makes it possible to monitor the currents and voltages between the different phases of the motor and ensure balanced, safe operation. Applying Kirchhoff's current law to the neutral point of the motor helps to understand how currents are distributed in a balanced or unbalanced system, and how this affects it. In a three-phase motor, the neutral point generally represents the connection point of the three stator windings. In symmetrical and balanced systems, this point is often earthed to improve safety and avoid any potential build-up in the neutral. This point becomes particularly important in the event of an unbalanced voltage between the phases. Kirchhoff's current law specifies that the sum of the currents flowing into a node is equal to the sum of the currents flowing out of that node, and this also applies to the neutral point of the system. In a three-phase induction motor, the sum of these currents must be zero in a balanced system [5]. This can be expressed as:

$$I_{sa} + I_{sb} + I_{sc} = 0 \qquad (1)$$

If there is an unbalance, this sum is no longer zero, resulting in a current in the neutral I_N, which can create a neutral voltage relative to the earth. In electrical systems, the neutral voltage is a critical parameter that can affect both the safety and efficiency of the installation. Neutral voltage is defined as the potential difference between the neutral point of the system and earth. The presence or absence of neutral voltage is largely influenced by the configuration of the neutral, whether bonded or un-bonded.

3.1 Neutral voltage calculation in a grounded neutral configuration

In a balanced system, the neutral current I_N is zero, which means the neutral voltage is also zero. The zero-sequence component is defined as the sum of the currents in the three-phase system. In a balanced system, this component represents the part of the current that is identical across all three phases, and it should theoretically be zero, as the currents in the three phases are equal and symmetrical. We have:

$$V_{so} = \frac{1}{3}\left(V_{sa} + V_{sb} + V_{sc}\right) \qquad (2)$$

$$V_n = V_{so} - \frac{1}{3}\left(\frac{d\varphi_{sa}}{dt} + \frac{d\varphi_{sb}}{dt} + \frac{d\varphi_{sc}}{dt}\right) \qquad (3)$$

If we assume that the value of V_{so} is zero in a healthy system due to the symmetrical distribution of the supply voltages, we can conclude that the neutral voltage will be:

$$V_n = -\frac{1}{3}\left(\frac{d\varphi_{sa}}{dt} + \frac{d\varphi_{sb}}{dt} + \frac{d\varphi_{sc}}{dt}\right) \qquad (4)$$

3.2 Neutral voltage behavior for bonded and un-bonded neutral configurations

The un-bonded neutral configuration presents significant risks to the safety, performance, and durability of equipment. In the absence of a ground reference, the neutral point of the system can fluctuate, creating floating neutral voltages, especially in the case of load unbalances. When the loads between phases are unequal, currents flow through the neutral, generating voltages that can reach dangerous levels for the machine. This leads to undesirable effects such as over-voltages, leakage currents, unbalances in the stator windings, and efficiency losses, increasing the risks of overheating and premature motor failure.

The neutral voltage V_N can be expressed as a function of the current in the neutral I_N and the impedance of the neutral Z_N. This can be written as:

$$V_N = I_N * Z_N \qquad (5)$$

The over-voltages due to a floating neutral can be expressed by the following equation:

$$V_O = I_O * Z_N \qquad (6)$$

(1) Z_N: Total circuit impedance (combining impedance of neutral and other system elements).
(2) V_N: Observed overvoltage.
(3) I_N: Overvoltage current.

In addition, leakage currents can be modeled as currents flowing through unwanted paths, such as the metal components of the machine:

$$I_L = \frac{V_N}{Z_L} \qquad (7)$$

(1) I_L: Leakage current.
(2) V_N: Line neutral voltage.
(3) R_L: Leakage path resistance.

Also, motor efficiency can be affected by the voltage difference between phases, leading to power losses.

$$P_{loss} = k * \Delta V^2 \qquad (8)$$

(1) P_{loss}: Power loss due to voltage unbalance.
(2) ΔV: Voltage difference between phases.
(3) k: Coefficient determined by machine type and level of unbalance.

4. EXPERIMENTAL METHODOLOGY AND DISCUSSIONS

The objective of this study is to investigate the impact of different neutral configurations (bonded vs. un-bonded neutral) on the detection and monitoring of internal and external unbalances in IM. Through a series of supervised experiments, we will compare the motor's performance under both configurations, focusing on the motor's ability to detect and respond to unbalances, its efficiency, stability, and longevity. The experimental methodology involves measuring key machine parameters at different points and identifying voltage and current unbalances across different neutral configurations.

Additional performance-related variables are also monitored. The experimental setup, as illustrated in Figure 1, consists of a three-phase squirrel-cage induction motor (model: FIMIT, 1.1 kW, 400 V, 50 Hz, 2-pole) and a dSPACE 1104 real-time control board for data acquisition and control. Current measurements are performed using five current transducers (model: LA 25-P, accuracy: ±0.9%), and voltage measurements are taken using four voltage transducers (model: LV 25-P, accuracy: ±0.9%). Motor speed is monitored using a Cheap GHS38 Motor Speed Sensor (360/500/1024 pulse incremental encoder, NPN open collector type).

Figure 1. Experimental setup for unbalanced supply voltage study

The motor is powered by two alternating current sources: one supplying the motor and the other dedicated to the sensors to ensure stable and isolated measurements. External unbalances are simulated by adjusting the power supply voltage levels variable resistance control (Figure 2), while internal unbalances are introduced by creating one or more broken rotor bars to assess their impact on motor performance. The experiments are conducted under two scenarios: external unbalance (voltage unbalance in the power supply) and internal unbalance (broken bar fault). The specified accuracy and sensitivity of the measurement equipment ensure reliable detection of unbalance conditions, while any limitations of the sensors are considered when interpreting the experimental results.

The experimental results presented in this study are subject to various sources of error, which were carefully considered and mitigated. Key sources include measurement inaccuracies, environmental factors, systematic biases, random noise, and human errors. For instance, current and voltage measurements were performed using high-precision sensors Lp 25-p and Lv 25-p respectively, with an accuracy level of 0.9%, as specified by the manufacturer. Environmental influences, such as temperature fluctuations, were minimized by conducting experiments in a controlled laboratory setting. Systematic errors, like sensor misalignment, were addressed through careful calibration, while random noise was reduced by averaging multiple measurements. Human errors were mitigated by automating data acquisition and validating results against theoretical predictions. These measures ensure the reliability and accuracy of the experimental findings, though some residual errors may remain.

Figure 2. Simulated unbalanced supply using variable resistance control

4.1 Experimental methodology for studying voltage unbalance

Voltage unbalance in a three-phase system occurs when the voltages of the three phases differ in magnitude or phase, leading to non-ideal operating conditions for connected equipment, including IM [21]. Causes of voltage unbalance include uneven load distribution, phase failures, transformer faults, the use of non-linear equipment like frequency converters, and variations in cable lengths or sizes. This unbalance negatively impacts motor performance by increasing phase currents, reducing torque, causing vibrations and noise, lowering efficiency, and potentially damaging motor components [22]. These effects can result in overheating, reduced motor lifespan, and higher maintenance costs. The voltage unbalance factor, which measures the difference between the phases, is expressed as a percentage and helps quantify the extent of the unbalance. According to IEC 60034-1 [2], a voltage unbalance factor of less than 1% indicates relatively balanced voltages. A high unbalance factor, however, can cause efficiency losses, increased energy consumption, premature equipment wear, and a shorter motor lifespan. Therefore, maintaining voltage unbalance limits is critical for ensuring the optimal performance of electrical installations and avoiding additional maintenance and energy costs. The equation for the Voltage Unbalance according to the IEC 60034-1 standard can be expressed as follows:

$$Voltage\,Unbalance\,(\%) = \frac{\max(V_1, V_2, V_3) - \min(V_1, V_2, V_3)}{\frac{1}{3}(V_1 + V_2 + V_3)} \times 100 \qquad (9)$$

(1) V_1, V_2, V_3: Are the line-to-line (or line-to-neutral) voltages of the three phases.

(2) $max(V_1, V_2, V_3)$: Is the highest voltage among the three phases.

(3) $min(V_1, V_2, V_3)$: Is the lowest voltage among the three phases.

(4) $\frac{1}{3}(V_1 + V_2 + V_3)$: Is the average voltage of the three

phases.

The Eq. (9) calculates the voltage unbalance percentage, which measures the degree of imperfection in a three-phase system. A voltage unbalance exceeding 2-3% is typically considered problematic for the proper functioning of IM and other sensitive equipment. The study is conducted in two parts: first, evaluating the behavior of the machine without faults, and second, assessing its performance with varying degrees of voltage unbalance under different neutral configurations. Using the MCSA method as previous studies [3, 4], the fault-specific frequencies will be identified. The experimental methodology for studying voltage unbalance is carried out by introducing a variable resistance upstream of the motor. Motor performance is then evaluated under these unbalanced conditions. These experiments aim to identify the impact of voltage unbalance on the motor's operational characteristics.

4.1.1 Bound neutral point condition for unbalance supply fault

Figure 3 illustrates two distinct operating conditions of the currents in an induction machine (IM). The first scenario depicts the machine's currents under healthy conditions, where all three phase currents are nearly equal in magnitude, indicating stable operation. A slight deviation is observed due to a minor disturbance in the mains supply, but this does not significantly impact the machine's overall performance. The second scenario represents the currents when one phase (specifically, the second phase) experiences a supply unbalance. In this case, the unbalance predominantly affects the current in the disturbed phase, while the currents in the remaining two phases remain relatively unaffected. This behavior is attributed to the use of an earthed neutral configuration, which helps contain the unbalance within the affected phase, preventing its propagation to the others.

Figure 4 illustrates the spectral analysis of stator currents in an induction machine under various operating conditions. Under healthy operating conditions (blue curve), the stator current spectrum is dominated by the fundamental supply frequency (fs), consistent with normal machine operation. The harmonic content is minimal, indicating a balanced power supply and optimal machine performance. In contrast, under unbalanced supply conditions (red and green curves), where the unbalance is deliberately introduced to the second phase, the spectra reveal significant deviations from the healthy state. Distinct frequencies associated with the supply unbalance clearly emerge and become more pronounced as the severity of the disturbance increases. These unbalance-related frequencies are typically characterized by the following relationship:

$$f_{unbalance} = f_s + 2*k*f_s \qquad (10)$$

where, "f_s" is the main supply frequency and "k" is a positive integer.

The magnitude of these characteristic frequencies exhibits a direct correlation with the severity of the unbalance, showing a clear variation as the fault level increases. The presence and amplification of these frequencies provide clear diagnostic indicators of supply disturbances and their impact on machine performance. The identification of these frequencies plays a pivotal role in diagnosing anomalies within electrical systems. Detecting these frequencies

facilitates the implementation of corrective measures to restore system balance and mitigate potential long-term damage to the machine. Moreover, the emergence and amplification of such frequencies may signal more profound underlying issues, including potential faults in the stator windings. Consequently, continuous monitoring of these spectral signatures is indispensable for ensuring the operational integrity and reliability of induction machines. This relationship enhances diagnostic precision and supports timely intervention, thereby safeguarding machine performance and longevity.

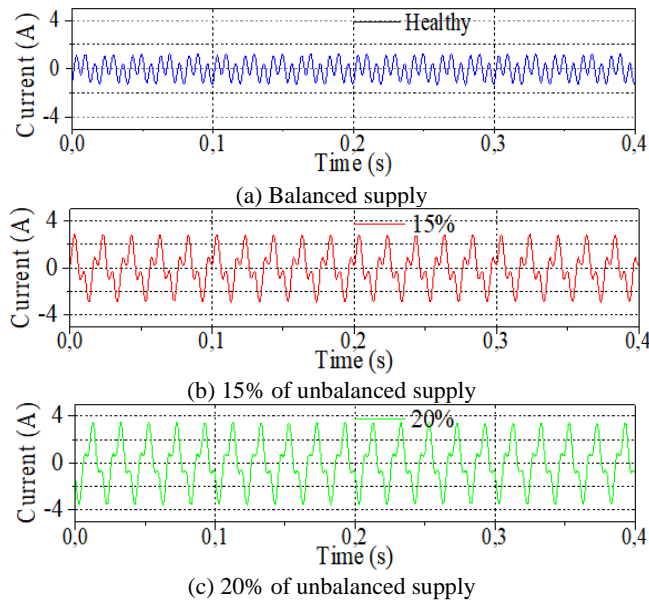(a) Balanced supply

(b) Unbalanced supply
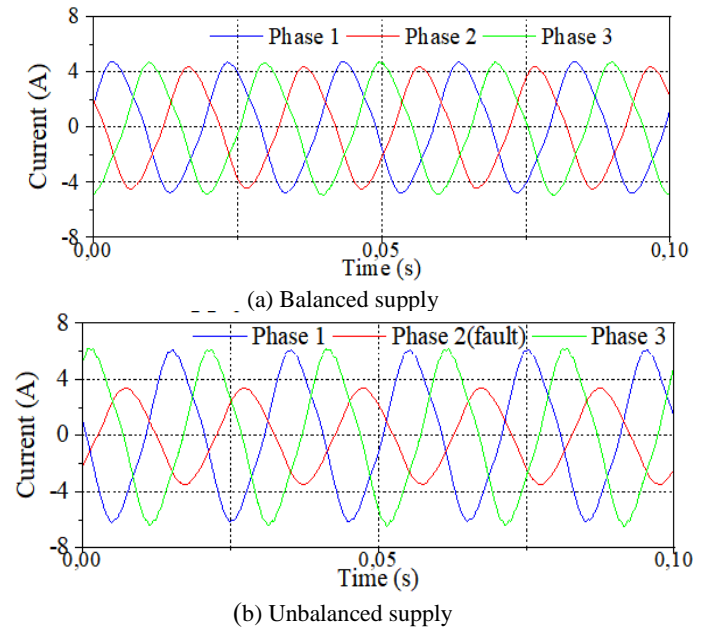
Figure 3. Stator currents under both balanced and unbalanced supply voltage conditions

Figure 5 illustrates the behavior of the line-to-neutral current under both balanced and unbalanced supply conditions, with varying degrees of unbalance. In a balanced system, the neutral current remains minimal and stable, reflecting the symmetry of the phase currents, which effectively cancel each other out, resulting in near-zero neutral current. However, under unbalanced conditions, the neutral current exhibits a significant increase in magnitude, directly correlated with the severity of the unbalance. The waveform also displays pronounced oscillations and distortions as the unbalance intensifies, a consequence of the asymmetric distribution of currents across the phases. The neutral current compensates for the excess or deficit in the affected phase, while the currents in the unaffected phases remain largely unchanged. In a balanced configuration, the neutral current is negligible due to the cancellation of balanced phase currents. However, when an unbalance occurs, the affected phase draws either more or less current than usual, and this discrepancy is reflected in the neutral current. The unaffected phases continue to operate normally, while the neutral current rises to offset the unbalance in the affected phase. This behavior highlights the importance of monitoring neutral current as a diagnostic tool for identifying supply unbalances, enabling timely corrective actions to maintain system stability and prevent potential damage to electrical infrastructure.

(a) Balanced supply

(b) 15% of unbalanced supply

(c) 20% of unbalanced supply
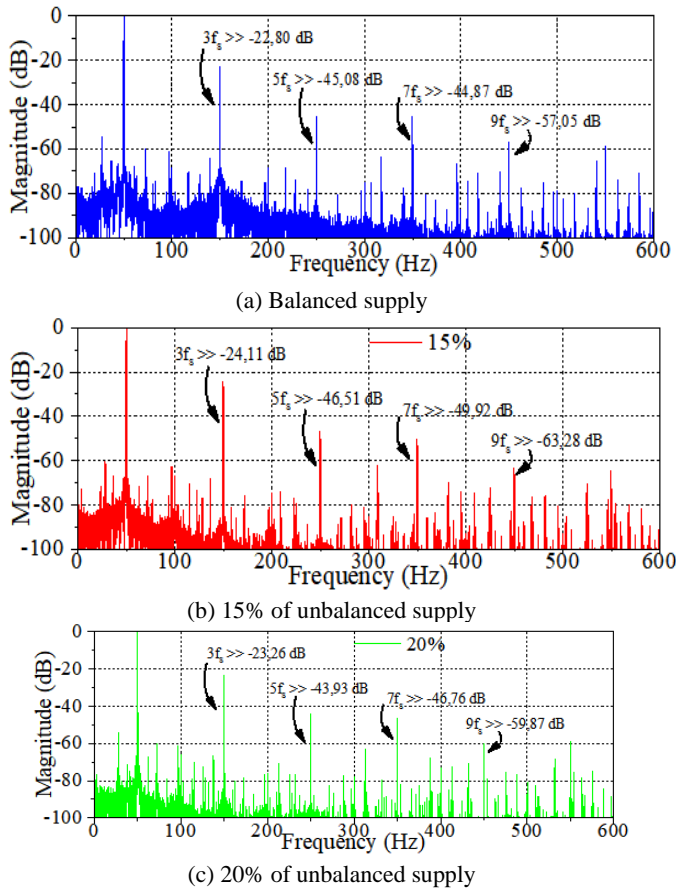
Figure 4. Stator current spectrum under healthy and unbalanced voltage conditions (15% and 20%)

(a) Balanced supply

(b) 15% of unbalanced supply

(c) 20% of unbalanced supply

Figure 5. Neutral line current under healthy and unbalanced supply conditions (15% and 20%)

Figure 6 depicts the behavior of harmonic components ($3f_s$, $5f_s$, $7f_s$, $9f_s$) as a function of unbalanced voltage severity and load torque variations. The blue curve represents the healthy operating condition, while the red, green, and magenta curves correspond to the first (F1), second (F2), and third (F3) degrees of unbalance voltage, respectively. The results indicate that the amplitudes of these harmonics fluctuate in response to changes in both load torque and fault severity.

However, these fluctuations do not follow a clear or consistent pattern, making it difficult to establish a definitive correlation between harmonic behavior and the progression of fault or load variations. This lack of a systematic trend complicates the interpretation of harmonic data as a reliable indicator of supply voltage unbalance.

Upon closer examination of Figure 6, certain trends can still be identified despite the complexity. Specifically, the 3rd harmonic ($3f_s$) exhibits a clear decrease in amplitude as the unbalance severity rises, particularly under lower load conditions. This behavior can be attributed to the introduction of zero-sequence components caused by supply voltage asymmetry, which becomes more pronounced in the presence of a neutral connection. As the load increases, the harmonic amplitude decreases overall, but differences between healthy and unbalanced scenarios remain noticeable.

Similarly, the 5th harmonic ($5f_s$) shows a peak in amplitude at medium load levels (approximately 25% to 50%), with higher fault severity leading to a distinct increase. The presence of negative-sequence components under unbalanced conditions contributes to this increase, affecting the motor's current waveform.

In contrast, the 7th harmonic (7fs) demonstrates a decreasing trend with increasing load, and the differences between healthy and faulty cases are less pronounced. This suggests that higher-order harmonics may be less sensitive to unbalance effects, likely influenced by nonlinear load interactions.

Lastly, the 9th harmonic (9fs) exhibits minimal variation and irregular behavior across different unbalance conditions and load levels, indicating limited diagnostic usefulness.

(a) Harmonic 3*fs

(b) Harmonic 5*fs

(c) Harmonic 7*fs

(d) Harmonic 9*fs
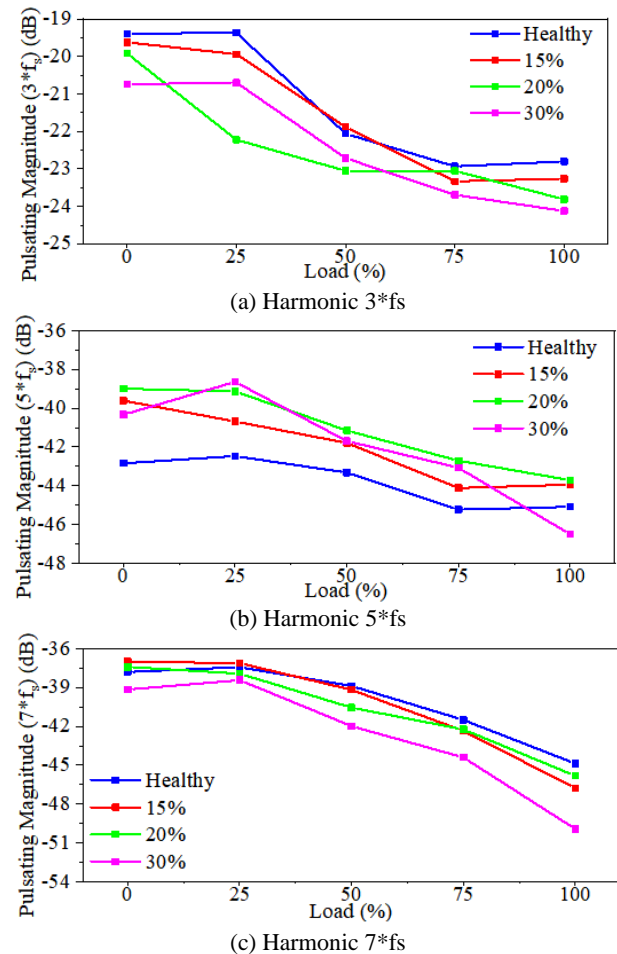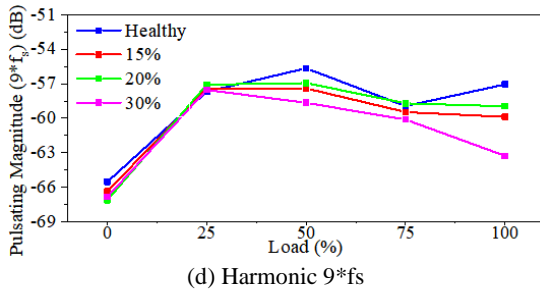
Figure 6. Harmonic amplitudes for varying percentages of unbalanced supply (15%, 20% and 30%)

4.1.2 Floating neutral point in case of unbalanced supply fault

Figure 7 demonstrates two distinct operational scenarios of the machine. The first scenario represents the machine under healthy operating conditions, where the three-phase currents demonstrate nearly identical magnitudes, consistent with balanced and normal operation.

The second scenario depicts the machine operating under a supply unbalance, specifically affecting one of the phases. In this case, the unbalance predominantly impacts the current of the affected phase, but it also induces secondary effects on the remaining phases.

This phenomenon is a direct consequence of the machine's isolated (unbonded) neutral connection configuration, which enforces the constraint that the sum of the three-phase currents must equal zero. Consequently, in an isolated neutral system, any unbalance in one phase is inherently compensated for by adjustments in the other phases to preserve the overall equilibrium of the system.

(a) Balanced supply

(b) Unbalanced supply
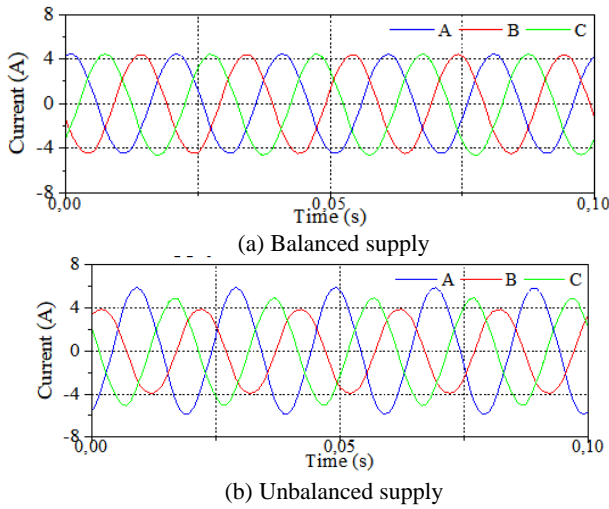
Figure 7. Stator currents under both balanced and unbalanced supply voltage conditions

This redistribution of current underscores the interconnected nature of phase currents in such systems and emphasizes the importance of considering neutral configuration when analyzing and diagnosing supply unbalances.

Figure 8 illustrates a spectral analysis of stator currents under various operating conditions in an unbounded neutral connection system. Under healthy operating conditions (blue), the stator current spectrum is predominantly characterized by

the fundamental supply frequency (f_s), indicative of normal system behavior. However, under unbalanced supply conditions (red and green), distinct frequencies associated with the unbalance become evident, with their prominence increasing in proportion to the degree of unbalance. These frequencies are typically represented as $f_{unbalance} = f_s + 2 * k * f_s$ where "k" is an integer. The emergence of these frequencies is a clear indicator of supply network unbalance, often resulting from voltage asymmetries.

The appearance of these unbalance-related harmonic components is a direct reflection of the asymmetry introduced in the supply network, and their amplitudes escalate with the severity of the unbalance. This behavior offers a clear diagnostic signal for identifying supply disturbances. However, it is important to note that the floating neutral configuration affects the distribution and intensity of these harmonics. Specifically, without a grounded neutral path, the imbalance-induced currents lack a low-impedance return path, leading to altered electromagnetic field distributions within the motor and affecting the visibility of certain harmonic components.

Moreover, the variation patterns observed in the harmonic amplitudes reveal valuable information about the system's sensitivity to fault types. In the floating neutral setup, the reduced damping effect may cause the harmonic components to fluctuate more sharply, especially under higher fault severity levels. This characteristic makes the spectral signatures more sensitive to minor unbalances but may also result in higher susceptibility to measurement noise.

The amplitude of these characteristic frequencies escalates with the severity of the unbalance, providing critical diagnostic information. This relationship not only enhances the precision of fault detection but also supports proactive measures to mitigate potential system disruptions. Continuous spectral analysis allows operators to assess not only the existence of voltage asymmetries but also their progression over time. Understanding how these harmonic patterns behave under different neutral point configurations, such as the floating neutral in this case, enables more accurate fault classification and supports the implementation of targeted corrective actions. Consequently, the relationship between harmonic behavior, fault severity, and neutral configuration enhances diagnostic precision and contributes significantly to the maintenance and reliability of electrical systems.

Figure 9 depicts the phase-to-neutral voltages under healthy and fault conditions (15%, 20% and 30%), highlighting the impact of increasing fault severity. Under normal operation, the voltage exhibits a stable sinusoidal waveform with consistent amplitude, reflecting balanced system conditions.

However, as faults intensify, the waveform undergoes progressive distortion, characterized by pronounced oscillations and greater amplitude fluctuations. These deviations correlate directly with the severity of the unbalance, providing a visual representation of fault progression. This behavior aligns with the spectral analysis presented in Figure 8, where fault-induced unbalances manifest as distinct frequency components. Together, these observations underscore the relationship between waveform distortion and spectral anomalies, offering complementary diagnostic insights. The ability to correlate time-domain voltage deviations with frequency-domain characteristics enhances the precision of fault detection and supports the

development of targeted mitigation strategies, ensuring system reliability under varying operational conditions.

(a) Balanced supply

(b) 15% of unbalanced supply

(c) 20% of unbalanced supply
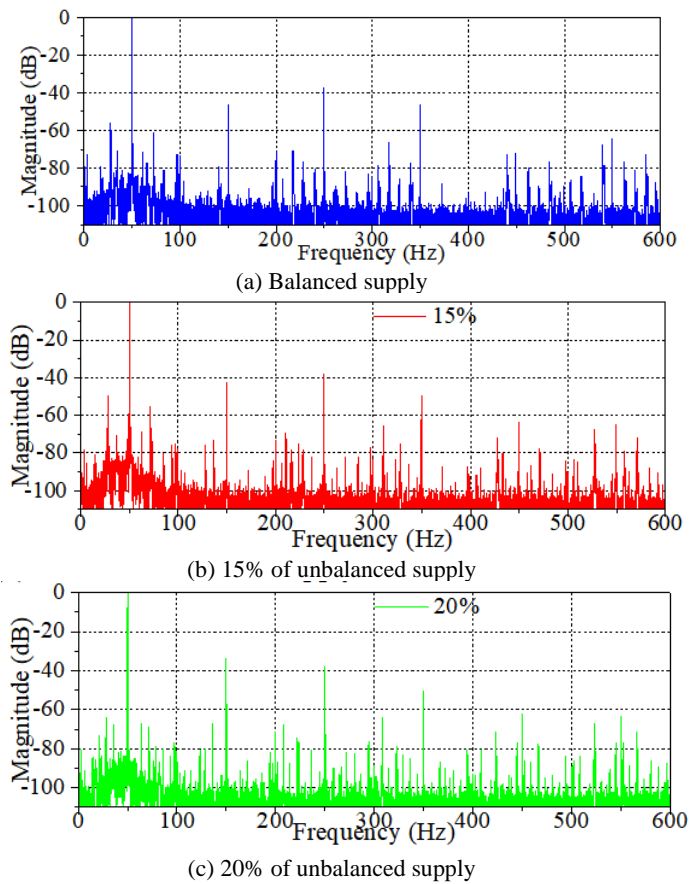
Figure 8. Stator current spectrum under healthy and unbalanced voltage conditions (15% and 20%)

(a) Balanced supply

(b) 15% of unbalanced supply
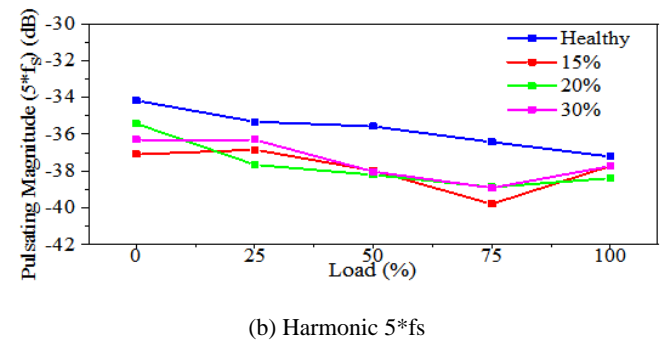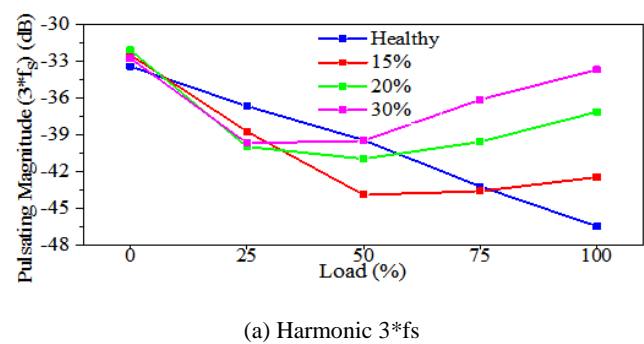
(c) 20% of unbalanced supply
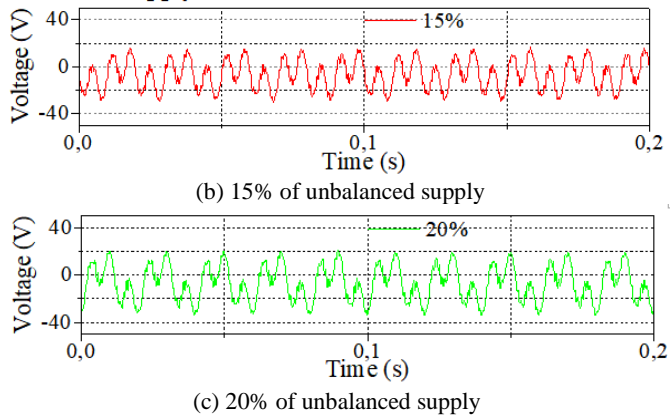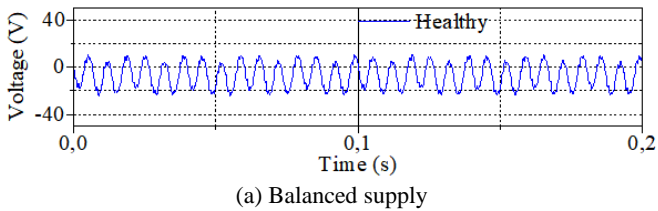
Figure 9. Neutral line voltage under healthy and unbalanced supply conditions (15% and 20%)

Figure 10 demonstrates the relationship between harmonic amplitudes, load conditions, and fault severity. A particularly notable trend is observed in the amplitude of the $3f_s$ harmonic, which systematically increases with variations in torque or fault degree.

This behavior strongly suggests the presence of an unbalanced supply voltage, as the harmonic response amplifies in tandem with the severity of the unbalance. These findings complement the observations from Figures 8 and 9, where fault-induced unbalances were shown to distort phase-to-neutral voltages and introduce characteristic frequency components in the stator current spectrum. The consistent increase in harmonic amplitudes under fault conditions further reinforces the diagnostic value of monitoring such spectral features. Additionally, the use of an un-bonded neutral connection in industrial systems enhances the detecting capability of these unbalances, thereby improving the reliability of diagnostic approaches. However, this configuration (Table 2) necessitates meticulous design and maintenance to address potential operational challenges. Collectively, these results highlight the importance of integrating time-domain and frequency-domain analyses to achieve robust fault detection and ensure system stability.

Table 2. Comparison between bonded and floating neutral in the event of voltage unbalance

Aspect	Bounded Neutral	Floating Neutral
Unbalanced current circulation	Possible, limits the effects of unbalances	Impossible, amplifies the effects
Floating voltages	Reduced	More important
Impact on equipment	Less pronounced, but heating of neutral	More severe, vibrations and overheating
Detecting the fault	Easy with classic protectors	More difficult, requires advanced devices

(a) Harmonic 3*fs

(b) Harmonic 5*fs

(c) Harmonic 7*fs

(d) Harmonic 9*fs
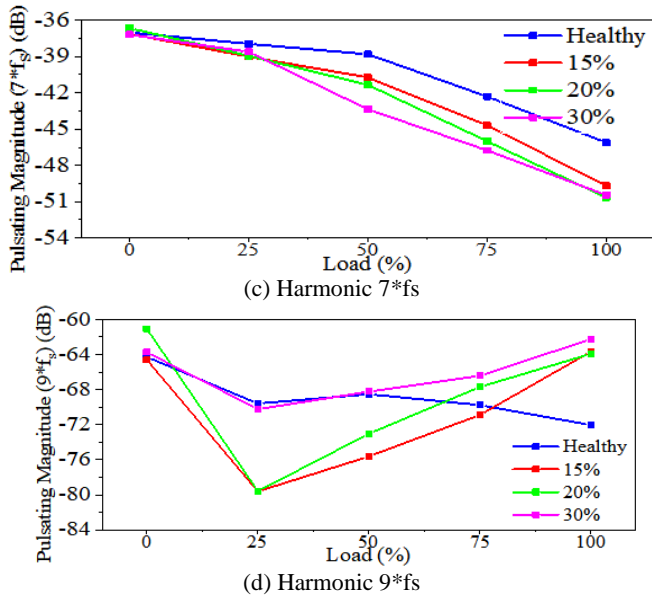
Figure 10. Harmonic amplitudes for varying percentages of unbalanced supply (15%, 20% and 30%)

4.2 Experimental methodology for studying broken rotor bar fault

A Broken Rotor Bar Fault (BRBF) in an induction motor occurs when one or more rotor bars fail, leading to current unbalances and reduced motor performance [4, 23]. Common causes include mechanical fatigue, electrical overloads, design flaws, and electromagnetic disturbances. The experimental methodology employed to study BRBF involves a rigorous and systematic approach to assessing the fault's impact on motor performance.

Initially, the motor is operated under normal conditions to establish baseline performance metrics, including torque and speed. To simulate a BRBF, controlled damage is deliberately induced, typically by causing a mechanical break in one or more rotor bars (Figure 11). Furthermore, the experimental setup incorporates the Motor Current Signature Analysis (MCSA) diagnostic technique, which enables a detailed investigation into how broken rotor bars affect the operational characteristics and efficiency of the motor.


Figure 11. Experimental setup for internal unbalance (broken rotor bar fault)

4.2.1 Bound neutral point condition for internal unbalance fault BRB

Figure 12 depicts three distinct operational states of the currents in an induction machine. Under normal operating conditions, the phase currents exhibit nearly identical amplitudes and waveforms, signifying healthy performance. However, when one or two rotor bars are damaged (represented by the second and third curves, respectively),

the current magnitudes show slight deviations. These changes are primarily due to the increased slip associated with the rotor bar fault, which induces minor asymmetries in the current waveforms.

(a) Healthy condition

(b) 1 BRB fault

(c) 2 BRB fault
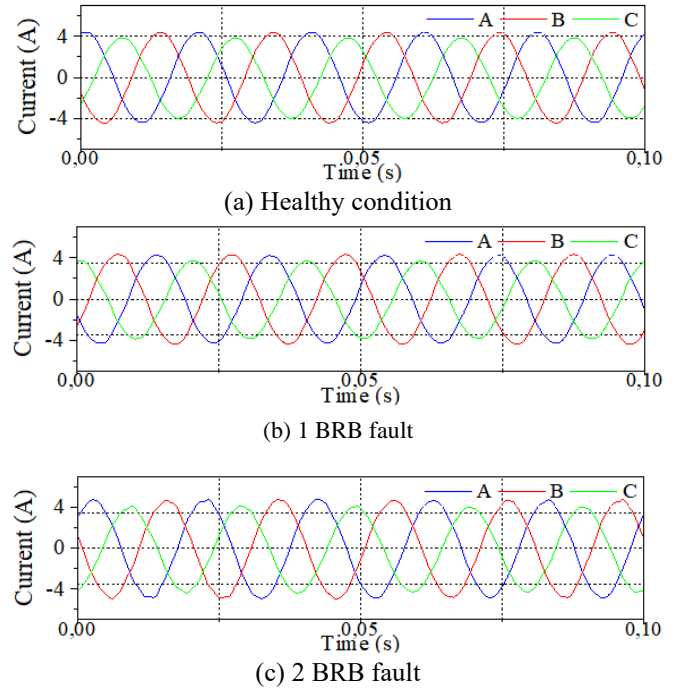
Figure 12. Stator currents curves under healthy and internal unbalanced (BRB) conditions

Figure 13 presents the line-neutral current waveform both in the healthy state and under various broken rotor bar faults (BRBF). In the healthy condition, the current waveform is smooth and consistent, indicating balanced operation. In contrast, when the machine experiences broken rotor bars, the line-neutral current curve exhibits significant changes, such as an increase in amplitude and distortion of the waveform. These alterations are a result of the elevated slip and mechanical unbalances introduced by the rotor bar damage.

(a) Healthy condition

(b) 1 BRB fault

(c) 2 BRB fault
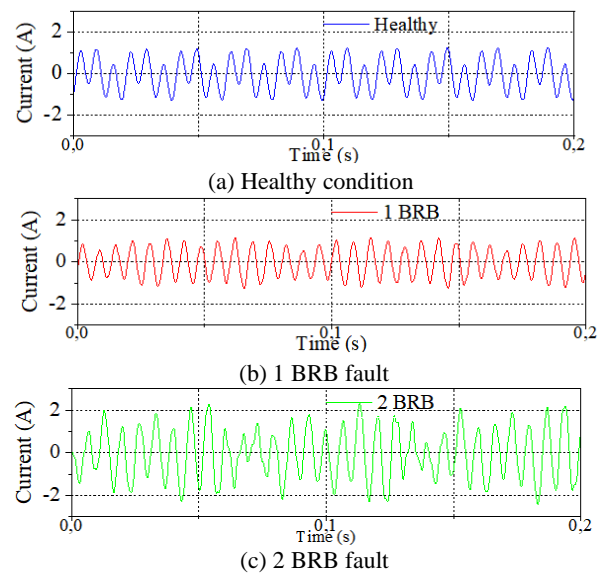
Figure 13. Line neutral current curve in healthy and internal unbalanced (BRB) conditions

Figure 14 presents a spectral analysis of the stator currents in IM under healthy and BRBF conditions in both no-load and full-load scenarios. In the healthy state (blue), the stator current spectrum is dominated by a peak at the fundamental supply frequency (f_s), characteristic of normal operation without faults. The rotating frequency (f_r) is also visible, further confirming the machine's proper functioning.

The spectrum contents minimal harmonic, indicating balanced and efficient machine performance. In contrast, under BRBF (red and green) the stator current spectrum shows significant deviations from the healthy state. Characteristic fault frequencies, indicative of rotor asymmetry, become prominent, highlighting the unbalance caused by the rotor fault. These frequencies can be expressed by the formula:

$$f_{BRB} = \left(1 \pm 2g\right) * f_s \qquad (11)$$

where, "g" represents the slip of the machine.

Furthermore, as the load increases, the fault frequencies shift further away from the fundamental frequency, reflecting the increased slip (g) under load conditions. This shift is accompanied by a proportional rise in the amplitude of these characteristic frequencies, signifying the severity and progression of the rotor fault. The amplitude increase becomes more pronounced with higher fault levels, offering a clear and quantifiable diagnostic marker for identifying BRBF. Additionally, the effect of load on these frequencies is evident, as they move further from the fundamental under full load due to the increased slip, highlighting the importance of considering load conditions in fault diagnosis.

(a) Healthy condition

(b) 1 BRB fault

(c) 2 BRB fault
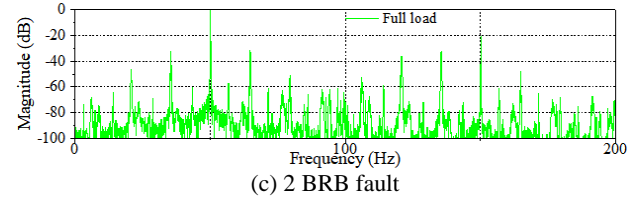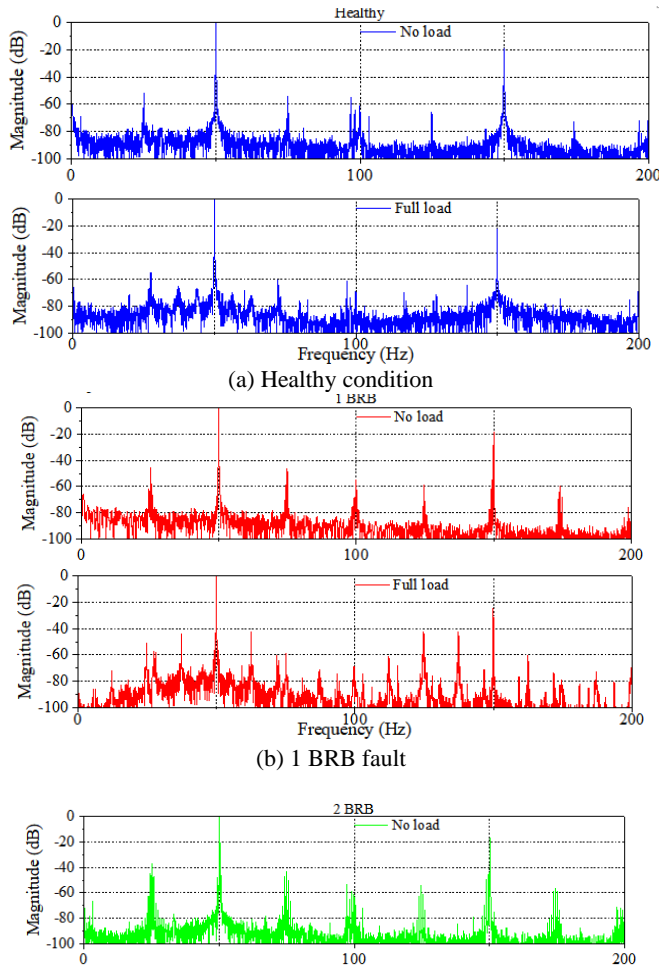
Figure 14. Stator current spectrum in healthy and internal unbalanced (BRB) conditions

It is also noteworthy that the presence of broken bars leads to asymmetric flux distribution within the rotor, which further contributes to the generation of sideband frequencies around the fundamental. These sidebands are reliable indicators of rotor faults, and their magnitude and frequency displacement serve as essential parameters in assessing fault severity. However, vibrations can distort the spectrum signals, introducing noise that complicates the accurate identification of fault-related frequencies. Therefore, careful signal filtering and advanced spectral analysis techniques are required to minimize external disturbances and ensure accurate detection of the rotor fault signatures.

4.2.2 Floating neutral point condition for internal unbalance fault BRB

Figure 15 presents the stator current waveforms for a system with a floating neutral connection. In the healthy state, the currents are balanced and symmetrical, exhibiting nearly identical amplitudes and waveforms. However, under broken rotor bar fault (BRBF) conditions, subtle deformations in the current waveforms are observed, indicating rotor damage.

Figure 16 shows the line-neutral voltage waveforms under both healthy and BRBF conditions. Following the fault, the voltage waveform displays slight distortions, asymmetries, and variations in amplitude. These changes are attributed to the increased slip and mechanical unbalances caused by the rotor damage.

(a) Healthy condition

(b) 1 BRB fault

(c) 2 BRB fault
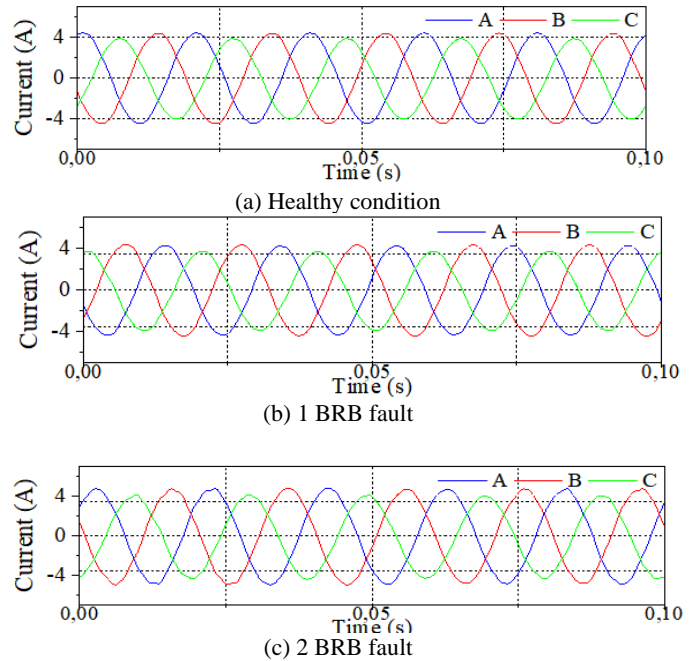
Figure 15. Stator currents curves under healthy and internal unbalanced (BRB) conditions

(a) Healthy condition

(b) 1BRB fault

(c) 2 BRB fault
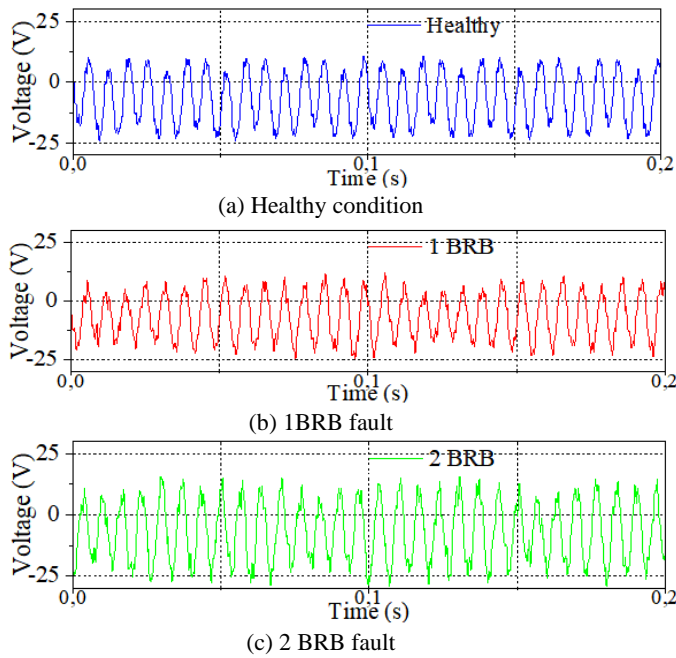
Figure 16. Line neutral voltage curve in healthy and internal unbalanced (BRB) conditions

These observations highlight the importance of monitoring both current and voltage to reliably detect rotor bar faults, especially since subtle anomalies in the waveforms can serve as early indicators of mechanical failures.

Figure 17 illustrates notable deviations, with characteristic fault frequencies linked to rotor asymmetry becoming more pronounced. These variations serve as indicators of rotor damage, underscoring the critical role of spectral analysis in fault detection. As the degree of unbalance increases, the amplitude of these characteristic frequencies also rises. The identified frequencies are:

$$f_{BRB} = (1 \pm 2g) * f_s \qquad (12)$$

A closer examination reveals that these fault-related sideband frequencies become increasingly prominent with the worsening of rotor faults, enabling early-stage detection and precise severity assessment. The amplitude growth of these sidebands is particularly useful for distinguishing between minor rotor defects and severe broken rotor bar conditions.

Based on the interpretation of Figure 17, it is also observed that in the presence of an un-bonded (floating) neutral, the vibration levels are generally lower compared to a bonded neutral system.

This reduction in vibration noise enhances the clarity of fault indicators in the stator current spectrum. As a result, the fault-related frequencies become more distinct and easier to detect, making the un-bonded neutral configuration particularly advantageous for identifying broken rotor bar faults.

(a) Healthy condition

(b) 1 BRB fault

(c) 2 BRB fault
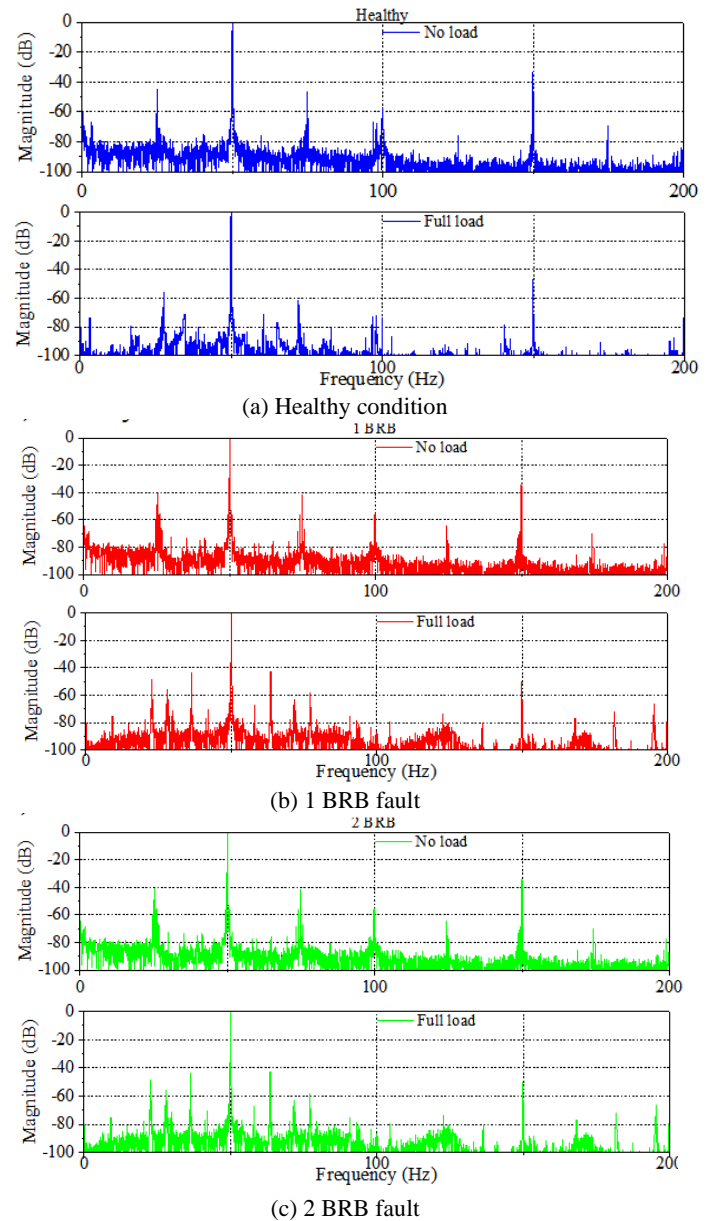
Figure 17. Line neutral voltage curve in healthy and internal unbalanced (BRB) conditions

Furthermore, the reduced interference in the floating neutral system minimizes the risk of external noise masking the fault signatures, allowing for a cleaner spectral analysis. This highlights the importance of considering the neutral configuration when designing fault detection schemes, as it directly impacts the accuracy and reliability of the diagnostic process. Continuous monitoring of these frequencies, combined with proper neutral configuration (Table 3), supports predictive maintenance strategies and enhances the longevity of IM.

Table 3. Comparison between bonded and floating neutral in the event of a bar break

Aspect	Bounded Neutral	Floating Neutral
Unbalanced current circulation	Possible, makes it easier to detect	Limited or non-existent
Floating voltages	Less pronounced	Larger, higher risk
Detecting the fault	Easy with conventional devices	More difficult, requires special systems
Overall impact	Easier to control, but may overheat	Hard to detect, risk of increased wear

5. CONCLUSION

This paper investigates the impact of neutral configuration on unbalance detection in IM. It demonstrates that earthed neutral systems enhance the motor's ability to detect and compensate for unbalances, whether external (power supply issues) or internal (rotor faults). Early detection reduces the risk of overheating, excessive vibration, and mechanical damage, thus minimizing unscheduled downtime and repair costs. The study also highlights the challenges associated with ungrounded neutral systems, where unbalances go undetected, increasing the risk of failure. It emphasizes the importance of effective monitoring and optimal neutral configuration to ensure reliable motor operation, with practical implications for the maintenance and longevity of industrial equipment. The experimental results also show that some neutral configurations improve the detection of external unbalances, while others are more sensitive to internal faults. For example, an earthed neutral improves the detection of voltage asymmetries, while isolated configurations better isolate the effects of internal faults. The paper also provides practical recommendations for selecting the appropriate neutral configuration based on operating conditions, as well as suggestions for improving the accuracy of unbalance detection systems. The findings have significant implications for predictive maintenance and reliability management of motors, helping to reduce repair costs and enhance the performance of industrial systems. In conclusion, the paper underscores the critical role of proper neutral configuration in supporting efficient fault detection and improving the reliability of IM.

While the experiments in this study were conducted on a specific type of induction motor under controlled laboratory conditions, the observed trends regarding the influence of neutral point configuration on fault detection are expected to be relevant to a wide range of industrial applications. However, motor characteristics such as size, design, and load variability can influence fault detection behavior. Therefore, further research involving different motor types and operating conditions is recommended to validate the generalizability of these findings and to refine the proposed recommendations for broader applicability.

REFERENCES

[1] Bahgat, B.H., Elhay, E.A., Sutikno, T., Elkholy, M.M. (2024). Revolutionizing motor maintenance: A comprehensive survey of state-of-the-art fault detection in three-phase induction motors. International Journal of Power Electronics and Drive Systems, 15(3): 1968-1989. https://doi.org/10.11591/ijpeds.v15.i3.pp1968-1989

[2] Von Meier, A. (2024). Electric power systems: Power electronics. In Electric Power Systems, John Wiley & Sons, pp. 405-424. https://doi.org/10.1002/9781394241033.ch14

[3] Constantin, A.I. (2019). Detection based on stator current signature of the single and combined short-circuit, broken bar and eccentricity faults in induction motors. In 2019 11th International Symposium on Advanced Topics in Electrical Engineering (ATEE), Bucharest, Romania, pp. 1-6. https://doi.org/10.1109/ATEE.2019.8724984

[4] Merabet, N., Babaa, F., Touil, A., Chibani, O.A.E. (2024). Combined-fault detection and diagnosis in induction motor using motor current signature analysis. In 2024 3rd International Conference on Advanced Electrical Engineering (ICAEE), Sidi-Bel-Abbes, Algeria, pp. 1-6. https://doi.org/10.1109/ICAEE61760.2024.10783215

[5] Touil, A., Babaa, F. (2022). Studying of unbalanced supply voltage effects on three-phase induction motor performances based on line neutral voltage analytical calculation. In International Conference on Electrical Engineering and Control Applications, Singapore, Singapore, pp. 455-467. https://doi.org/10.1007/978-981-97-0045-5_41

[6] Touil, A., Babaa, F., Kratz, F., Bennis, O. (2024). Bearing fault diagnosis in induction machines based on electromagnetic torque spectral frequencies analysis. Journal Européen des Systèmes Automatisés, 57(1): 255-261. https://doi.org/10.18280/jesa.570124

[7] Alvarado-Hernandez, A.I., Zamudio-Ramirez, I., Jaen-Cuellar, A.Y., Osornio-Rios, R.A., Donderis-Quiles, V., Antonino-Daviu, J.A. (2022). Infrared thermography smart sensor for the condition monitoring of gearbox and bearings faults in induction motors. Sensors, 22(16): 6075. https://doi.org/10.3390/s22166075

[8] Tabasi, M., Ojaghi, M., Mostafavi, M. (2021). Analyzing vibration as a useful domain for getting bearing fault signals in induction motors. International Journal of Engineering, 34(8): 2010-2020. https://doi.org/10.5829/ije.2021.34.08b.22

[9] Okwuosa, C.N., Akpudo, U.E., Hur, J.W. (2022). A cost-efficient MCSA-based fault diagnostic framework for SCIM at low-load conditions. Algorithms, 15(6): 212. https://doi.org/10.3390/a15060212

[10] Al-Musawi, A.K., Anayi, F., Packianather, M. (2020). Three-phase induction motor fault detection based on thermal image segmentation. Infrared Physics & Technology, 104: 103140. https://doi.org/10.1016/j.infrared.2019.103140

[11] Jalilian, A., Roshanfekr, R. (2009). Analysis of three-phase induction motor performance under different voltage unbalance conditions using simulation and experimental results. Electric Power Components and Systems, 37(3): 300-319. https://doi.org/10.1080/15325000802454476

[12] Gundewar, S.K., Kane, P.V. (2021). Condition monitoring and fault diagnosis of induction motor. Journal of Vibration Engineering & Technologies, 9: 643-674. https://doi.org/10.1007/s42417-020-00253-y

[13] Siddiqui, K.M., Giri, V.K. (2012). Broken rotor bar fault detection in induction motors using wavelet transform. In 2012 International Conference on Computing, Electronics and Electrical Technologies (ICCEET), Nagercoil, India, pp. 1-6. https://doi.org/10.1109/ICCEET.2012.6203753

[14] Kumar, R.R., Andriollo, M., Cirrincione, G., Cirrincione, M., Tortella, A. (2022). A comprehensive review of conventional and intelligence-based approaches for the fault diagnosis and condition monitoring of induction motors. Energies, 15(23): 8938. https://doi.org/10.3390/en15238938

[15] Allal, A., Khechekhouche, A. (2022). Diagnosis of induction motor faults using the motor current normalized residual harmonic analysis method.

International Journal of Electrical Power & Energy Systems, 141: 108219. https://doi.org/10.1016/j.ijepes.2022.108219

[16] Yang, P.H., Li, Y., Liu, L.G., Dong, X.L., Zhang, J.J. (2019). Optimal placement of grounding small resistance in neutral point for restraining voltage fluctuation in power grid caused by geomagnetic storm. IET Generation, Transmission & Distribution, 13(8): 1456-1465. https://doi.org/10.1049/iet-gtd.2018.6310

[17] Santiago, F., Bento, F., Cardoso, A.J.M., Gyftakis, K.N. (2019). Thermal analysis of a directly grid-fed induction machine with floating neutral point, operating under unbalanced voltage conditions. Electric Power Components and Systems, 47(11-12): 1060-1076. https://doi.org/10.1080/15325008.2019.1659451

[18] Schachinger, P., Albert, D., Renner, H. (2023). Reduction of geomagnetically induced current impacts by optimized neutral point connections. IET Generation, Transmission & Distribution, 17(17): 3984-3992. https://doi.org/10.1049/gtd2.12957

[19] Salehi Arashloo Arashloo, R., Romeral Martínez, J.L., Salehifar, M., Sala Caselles, V. (2014). Impact of neutral point current control on copper loss distribution of five phase PM generators used in wind power plants.

Advances in Electrical and Computer Engineering, 14(2): 89-96. https://doi.org/10.4316/AECE.2014.02015

[20] Maheshwari, R., Munk-Nielsen, S., Busquets-Monge, S. (2011). Neutral-point current modeling and control for neutral-point clamped three-level converter drive with small DC-link capacitors. In 2011 IEEE Energy Conversion Congress and Exposition Phoenix, AZ, USA, pp. 2087-2094. https://doi.org/10.1109/ECCE.2011.6064044

[21] Hussain, M., Memon, T.D., Hussain, I., Ahmed Memon, Z., Kumar, D. (2022). Fault detection and identification using deep learning algorithms in induction motors. CMES-Computer Modeling in Engineering & Sciences, 133(2):436-470. https://doi.org/10.32604/cmes.2022.020583

[22] Noussaiba, L.A.E., Abdelaziz, F. (2024). ANN-based fault diagnosis of induction motor under stator inter-turn short-circuits and unbalanced supply voltage. ISA Transactions, 145: 373-386. https://doi.org/10.1016/j.isatra.2023.11.020

[23] Halder, S., Bhat, S., Zychma, D., Sowa, P. (2022). Broken rotor bar fault diagnosis techniques based on motor current signature analysis for induction motor—A review. Energies, 15(22): 8569. https://doi.org/10.3390/en15228569